CHEMISTRY OF MATERIALS

Article

Label-free and selective single-molecule bioelectronic sensing with a millimeter-wide self-assembled monolayer of anti-immunoglobulins

Eleonora Macchia, Amber Tiwari, Kyriaki Manoli, Brigitte Holzer, Nicoletta Ditaranto, Rosaria Anna Picca, Nicola Cioffi, Cinzia Di Franco, Gaetano Scamarcio, Gerardo Palazzo, and Luisa Torsi

Chem. Mater., **Just Accepted Manuscript** • DOI: 10.1021/acs.chemmater.8b04414 • Publication Date (Web): 02 Jan 2019

ACS Publications

is published by the American Chemical Society. 1155 Sixteenth Street N.W., Washington, DC 20036

Label-free and selective single-molecule bioelectronic sensing with a millimeter-wide self-assembled monolayer of anti-immunoglobulins

Eleonora Macchia,[a] Amber Tiwari,[a] Kyriaki Manoli,[a] Brigitte Holzer,[a] Nicoletta Ditaranto,[a] Rosaria Anna Picca,[a] Nicola Cioffi,[a] Cinzia Di Franco,[b] Gaetano Scamarcio,[c],[b] Gerardo Palazzo,[a],[d] and Luisa Torsi *[a],[d]

[a] Dipartimento di Chimica - Università degli Studi di Bari "Aldo Moro" - Bari (I)

[b] CNR - Istituto di Fotonica e Nanotecnologie, Sede di Bari (I)

[c] Dipartimento di Fisica "M. Merlin" - Università degli Studi di Bari – "Aldo Moro" - Bari (I)

[d] Centre for Colloid and Surface Science - Università degli Studi di Bari "Aldo Moro" Bari (I)

*e-mail: luisa.torsi@uniba.it

ABSTRACT: Immunoglobulin M (IgM) single-molecule and label-free detection is demonstrated, for the first time, by means of an electrolyte-gated thin-film transistor. The sensor integrates a millimeter-wide self-assembled monolayer (SAM) that includes trillions of anti-IgM capturing proteins. This adds generality to the already introduced Single-Molecule with a Transistor (SiMoT) platform. Besides the extremely high sensitivity, the SAM confers to the SiMoT bioelectronic sensor a high selectivity that is here assessed by measuring the differential responses of the IgM or the immunoglobulin G (IgG) cognate biomarkers mutually interacting with anti-IgM or anti-IgG capturing SAMs. At the same time, no response to IgG or IgM is measured with the anti-IgM or anti-IgG SAM, respectively. The SiMoT technology is known to exploit the hydrogen bonding network present in the SAM. In this paper, further elements supporting the model of this network enabling single-molecule sensitivity is provided by demonstrating that, once this electrostatic connecting element is removed, the sensing is suppressed. It also provides a plausible explanation of the wide-field single-molecule sensing mechanism in terms of amplified field-effect response and propagation of electrostatic domains associated with the electrostatic hydrogen bonding network. Future possible applications to low-cost early detection of infection diseases can be envisaged.

INTRODUCTION

The rising interest in single-molecule detection stems from the importance to face the ultimate challenge of counting each molecule in a solution, but also from the relevance of studying the wide spectrum of subtle differences characterizing each single-molecule interaction. The sensing of single-events opens in fact, to the study of rarer events that are otherwise lost in the background noise when the average most probable response of a population of countless molecules, is measured. From the applications perspective, the aim is to develop a digital and low-cost technology that, by tracking a target biomarker with single-molecule precision, can quantify the transition of a biological organism from being *healthy* to being *diseased*. This can open to the possibility of achieving the earliest possible diagnosis. The better and better performances reached by the single-molecule sensing devices has led to the development of different quantification technologies. Gooding and Gaus have nicely categorized them by focusing on the interaction cross-section.[1] Label-free single-molecule detection has up until now been achieved with nanometre-sized transducers. This is here addressed as a *near-field* measurement as, in analogy with scanning probe microscopies, the probe apex size is comparable to that of the probed object.[2] A paradigmatic example is the single DNA strand detection by means of a few bio-probes attached to defect point on a single-nanotube transistor.[3] Due to the very small interaction cross-section, this approach does not allow to measure a single molecule into a bulk milieu in a reasonably short time-frame.[4] The *wide-field capturing* overcomes this issue by means, for instance, of a large number of beads, functionalized with the capturing antibodies, that are dispersed into the volume containing the few bio-markers to be captured and analyzed. In the exemplary case of the digital enzyme-linked immunosorbent assay,[5] the beads that have captured the biomarkers, are labelled with a second antibody and a fluorophore and are dispersed onto an array offering wells where zero or one bead can be hosted. Finally, the fluorescent wells in the array are counted. Although much less explored, the *wide-field measurements,* in which single molecules are sensed by means of a detecting interface orders of magnitude larger, are in principle the most effective. In this case the critical aspect is measuring a signal that is sufficiently larger than the noise level or, equivalently, that falls beyond the limit of detection.[6] While single-molecule, label-free sensing has

been carried out so far only with near-field measurements,[7] our group has recently demonstrated the first proof-of-concept of a label-free Single Molecule detection of immunoglobulin G (IgG) with a large (*wide-field*) Single Molecule with a Transistor (SiMoT) sensor.[8,9] The present study is an important step further in assessing the wider applicability of the SiMoT platform. Here, Immunoglobulin M (IgM) biomarkers single-molecule, label-free detection is demonstrated, for the first time, with a SiMoT electrolyte-gated thin-film transistor.[10] Moreover, both IgM and IgG cognate ligands selective detection is proven by means of self-assembled monolayers (SAMs) of anti-IgM or anti-IgG capturing molecules integrated by covalent attachment to the gate of a SiMoT transistor. While both IgM or IgG are detected at the single-molecule limit, with anti-IgM or anti-IgG SAMs respectively, no response to IgG or IgM is recorded in the whole inspected range of concentrations. The SAMs are also endowed with a hydrogen bonding network and evidences are here provided to further support the model of a collaborative amplification effect triggered by this network. To this end a SAM comprising 2-mercaptoethanol (2-ME) instead of the previously engaged 3-mercaptopropionic acid (3-MPA), was used proving that no sensing could be recorded in this case. Moreover the role of the field-effect capacitive coupling is detailed by showing its relevance in reaching extremely high sensitivities. At the same time an analytical model based on Poisson statistics gives an excellent reproduction of the experimental sensing dose curves and supports the model of the H-bonding network enabling the propagation of the single binding event effect to wider electrostatic domains. Possible applications can be envisaged in the early detection of diseases such as dengue virus infection, where both IgG and IgM are arrayed.[11]

EXPERIMENTAL SECTION

Materials: Anti-human Immunoglobulin G and anti-human Immunoglobulin M both produced in goat are polyclonal antibodies. Human IgG (~150 kDa) and human IgM (~950 kDa) affinity ligands are isolated from pooled normal human serum. Bovine serum albumin (BSA) has a molecular weight of 66 kDa. Phosphate buffered saline (PBS) was prepared according to the supplier`s instruction by dissolving one tablet in 200 mL of water (HPLC-grade) yielding a 0.01 M phosphate buffer, 0.0027 M potassium chloride and 0.137 M sodium chloride, pH 7.4, at 25 °C. All the reagents were purchased from Sigma-Aldrich and used with no further purification.

SiMoT electrolyte gated thin-film transistor fabrication: The SiMoT sensors have been fabricated starting from a highly n-doped silicon substrate, covered by thermally grown SiO_2. Source (S) and drain (D) interdigitated electrodes were photo-lithographically defined on a Si/SiO_2 substrate. Ti/Au (5/50 nm) films were deposited by electron-beam evaporation. The channel length is 5 μm and the geometrical channel width is 10.560 μm while the effective channel area, estimated by impedance spectroscopy measurements, is $6.4 \cdot 10^{-3}$ cm^2.[10] A Poly(3-hexylthiophene-2,5-diyl), P3HT, solution (2.6 $mg \cdot ml^{-1}$ in chlorobenzene) filtered with 0.2 μm filter was spin-coated at $2 \cdot 10^3$ r.p.m. for 20s and annealed at 90°C for 15 min, across and above the S and D interdigitated electrodes. A polydimethylsiloxane well was glued across the interdigitated channels area and filled with 300 μl of water (HPLC-grade) acting as gating medium. A gold L-shaped lamina with an area of about $3 \cdot 10^{-2}$ cm^2 served as gate (G) electrode.

Gate bio-functionalization protocol: The gold lamina was cleaned in a *piranha* solution (H_2SO_4 and H_2O_2, 3:1 v/v) for 20 min and immersed in boiling water for 10 min and subsequently treated with ozone for 10 min. The details of the chemical SAM (chem-SAM) functionalization protocol on the gold surface is reported elsewhere.[12] Here the most relevant features of the chemical functionalization procedure are summarized: The chem-SAM on the gold surface comprises a layer of mixed alkanethiols terminating with carboxylic functionalities. To this end, a 10 mM solution consisting of 10:1 molar ratio of 3-MPA and 11-mercaptoundecanoic acid (11-MUA) was prepared in ethanol. The cleaned gold surface was immersed in the 3-MPA and 11-MUA solution and kept in the dark under constant N_2 flux for 18 h at 22 °C. Alternatively, a mixture of 2-ME and 11-MUA at 10:1 relative concentration, were also used. The carboxylic groups were activated afterwards in a 200 mM -ethyl-3-(3-dimethylaminopropyl)-carbodiimide (EDC), and 50 mM N-hydroxysulfosuccinimide sodium salt (sulfo-NHS) aqueous solution for 2 h at 25 °C. Anti-IgG and anti-IgM were covalently attached on the chem-SAM as reported elsewhere.[14] The gate comprising the activated chem-SAM is immersed into an anti-IgM or anti-IgG phosphate buffer saline (PBS) solution for 2 h at 25 °C. The solution was composed of 0.7 μM (0.1 $mg\ ml^{-1}$) of anti-IgM or anti-IgG and 10 mM (KCl 2.7 mM and 137 mM NaCl) of PBS at a pH of 7.4 and an ionic-strength (i_s) of 162 mM. Afterwards, to saturate the unreacted sulfo-NHS groups, the anti-IgM (or amti-IgG) SAM was further treated with ethanolamine 1 M in PBS 10 mM for 1 h at 25 °C. Afterword, the bio-functionalized gate was immersed in a 1.5 μM (0.1 $mg \cdot ml^{-1}$) BSA solution in PBS 10 mM for 1 h at 25 °C. The anti-IgG was also deposited by physical adsorption directly on the gold lamina. To this end, the cleaned gate is immersed in the elicited anti-IgG PBS solution for 2 h at 25 °C and subsequently into the BSA solution in PBS for 1 h at 25 °C.

Sensing measurements: The transistor current-voltage curves were measured with a semiconductor parameter analyzer equipped with a probe station, in air and at RT (20-22 °C). Before proceeding with the sensing measurements, the device was let to stabilize in deionized water for about 12-24 hours after deposition. Afterwards, the I_D was further stabilized by cycling the measurement of the transfer curve of the P3HT SiMoT comprising a clean bare gold gate, until the last three current traces overlapped. A functionalized gate was then incubated (at RT and in the dark) for 10 min in 100 μl of PBS. The functionalized gate was removed from the PBS solution, washed thoroughly with HPLC water, mounted on the SiMoT (exactly replacing the bare gold-gate previously used) and a new transfer characteristic was registered. After the measurement of a stable I_0 base line, the same gate was immersed and incubated for 10 min in 100 μl of the PBS standard-solutions of the ligands (IgG or IgM) with nominal concentrations ranging from 6 zM to $60 \cdot 10^8$ zM. After incubation in each of the PBS standard-solutions of IgG or IgM starting from the more diluted one, the SAM was washed thoroughly with water (HPLC grade) to remove the unreacted ligands and further I-V transfer curves were measured. All the

data points are averaged over three replicates. The resulting reproducibility error is computed as the relative standard deviation. Further three anti-IgG (or anti-IgM) functionalized gates were employed to measure the IgM (or IgG) negative control dose-curves as well.

RESULTS

In **Figure 1A** the SiMoT electrolyte gated field-effect transistor structure is introduced. It comprises a resistor composed of a P3HT organic semiconductor deposited by spin-coating across and above the source (S) and drain (D) interdigitated electrodes. The resistor is located at the bottom of a sealed well that is filled with deionized water (resistivity>18 MΩ). The gate electrode is a gold rigid lamina with an active area of ~ 0.3 cm^2 that stably hangs, while in contact with the water in the well, at a distance of ~ 4 mm from the P3HT surface. The P3HT capacitance per unit area in water was measured to be 11 $\mu F/cm^2$,[10] so the whole channel capacitance is ~ 70 nF. The overall resistor is several millimetres in size and is fabricated by large-area scalable procedure. A picture of the SiMoT device is available at reference [9]. In **Figure 1B** the structure of the chem-SAM is detailed, while in **Figure 1C** both the chem-SAM and the bio-SAM, forming the capturing SAM, are depicted. Typical P3HT SiMoT output characteristics where the drain current (I_D) is measured as a function of V_D at different gate voltages V_G are shown **Figure 1D**. The gate leakage current I_G, in the same V_G range, is about three orders of magnitude lower than I_D (*vide infra)*. The curves were measured in the forward and reverse mode to prove that a negligible hysteresis is present. Low hysteresis and gate leakage are measured by tuning the organic thin-film transistor operating voltage ranges away from the potentials where electrochemical processes occur. In such operational condition the P3HT SiMoT stability can be quite high. This is proven in **Figure 1S**, where the I_D level changes by less than 6% during several hours of operation. Importantly, a P3HT SiMoT can exhibit such a high stability when it is let to stabilize in deionized water for about 12-24 hours after deposition before use in sensing measurements.

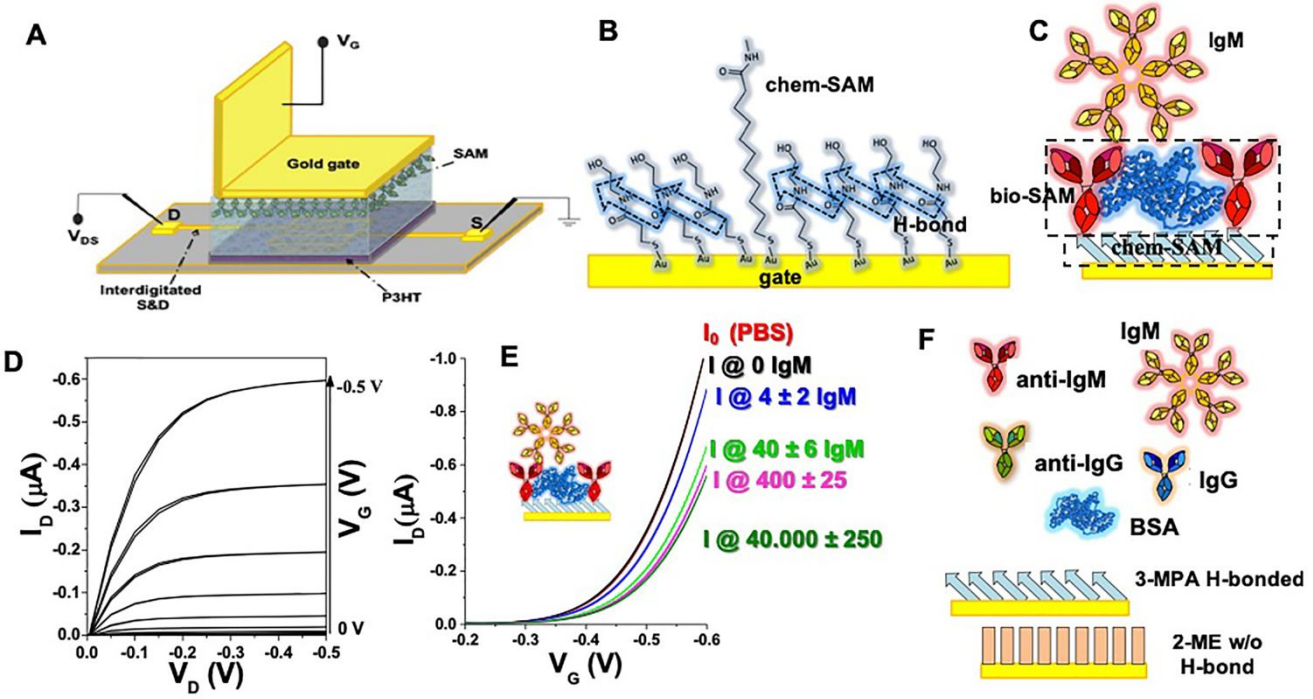

Figure 1. A - The three-dimensional schematic structure of the SiMoT sensor. **B -** Detailed structure of the chem-SAM, composed of 3-MPA and 11-MUA, evidencing the H-Bonds connecting two contiguous chains with hollow blue arrows. **C -** Sketch of an anti-IgM functionalized gold gate comprising both the chem-SAM (blue arrows) and the bio-SAM. **D -** Output characteristics (I_D vs. V_D, with V_G ranging from 0 V to -0.5 V in steps of -0.1 V) measured with an L-shaped gold lamina gate. **E -** SiMoT sensing transfer characteristics (I_D vs. V_G at V_D=-0.4 V) along with the sketch of the bio-functionalized gate. The chem-SAM is featured by arrows schematically indicating the dipole moments of the H-bond network. The red-curve corresponds to the anti-IgM functionalized gate incubated in the sole PBS solution. The same gate is further exposed, in sequence, to PBS standard-solutions of IgM at concentrations of: 6 zM (black-curve), (6±3)·10 zM (blue-curve), (6±1)·10^2 zM (light-green-curve), (6.7±0.1)·10^3 zM (magenta-curve) and (6.67±0.01)·10^6 zM (dark-green-curve). The number of IgM molecules found (the error bar is one sigma of the Poisson sampling) at each concentration in 100 μL are given in the figure. **F -** Legend of the symbols that are used in this article to address the proteins studied, along with the symbols used to address a chem-SAM endowed and not with an H-bond network.

The core of the bioelectronic sensor is the SAM of biological capturing elements that are covalently attached to the gate. As anticipated, a mixed SAM of carboxylic terminated alkanethiols, namely: 3-MPA and 11-MUA at 10:1 relative concentration is the chem-SAM layer (**Figure 1B**). Alternatively, a mixture of 2-ME and 11-MUA were also

used. The carboxylic groups are activated by means of EDC/sulfo-NHS chemistry before either the anti-IgM or the anti-IgG capturing antibodies are covalently attached to the chains. After the conjugation of the capturing antibodies (anti-IgM or anti-IgG) to the activated chem-SAM, ethanolamine is added to block the unreacted activated carboxylic groups. The amides groups that are formed originate hydrogen bondings connecting the oxygen of the amide group in one chain to the hydrogen of the amide group of the neighbouring one. A dipole moment is associated to each H-bond, illustrated in **Figure 1B** as hollow blue arrows, hence an electrostatic network is generated. This dipole moment, being ~ 3.7 D, is larger than the Au-S one (1-2 D).[13] Hence it affects more markedly the electrostatic interactions in the chem-SAM. It is reasonably assumed that mostly the 3-MPA chains are connected by this network as the 11-MUA ones are too sparse to form a network themselves.[10] When the 2-ME is used, as no carboxylic groups are present, no H-bond network is generated. As a last step, BSA is let to physisorb on the bio-functionalized gate to minimize non-specific binding. The capturing antibodies plus the BSA proteins form the bio-SAM, while the chem-SAM and the bio-SAM form the SAM. The anti-IgM bio-SAM on the gate is schematically illustrated in **Figure 1C**, while in **Figure 1F** a legend for all the sketches used in given. The whole comprehensive description of the bio-functionalization protocol is provided elsewhere.[10,12,14]

The amount of anti-IgG and anti-IgM capturing proteins immobilized on the gate was estimated by measuring the surface plasmon resonance (SPR) shift $\Delta\theta$ occurring when either the anti-IgG or the anti-IgM capturing proteins are conjugated to the activated chem-SAM (**Figure 2S**). According to the literature,[15,16] the surface coverage per unit area is estimated as $\Gamma=\Delta\theta*550$ ng·cm^{-2}. For anti-IgG and anti-IgM, Γ was 283±17 ng/cm^2 and 326±20 ng/cm^2, respectively. Taking into account the actual gate electrode area (0.3 cm^2) and the weight of a single anti-IgG or anti-IgG (~10^{-19} g), the average total number of binding-sites attached to the gate is ~10^{12}. This proves how the SiMoT gate bio-functionalization procedures results into an extremely highly packed SAM of capturing proteins. Such an extremely large number of capturing proteins largely improves the cross-section of one bio-marker interacting with a capturing ligand attached to the gate. Importantly, also when the chem-SAM is composed of the 2-ME and the 11-MUA, the same number of capturing proteins is attached to the gate as proven by the SPR experiment in **Figure 3S**. This implies that the capturing proteins are mostly attached to the 11-MUA. Despite the high density of capturing proteins, the SiMoT SAM was proven to be permeable to small ions, as demonstrated in **Figure 4S.** Here both the anti-IgM or anti-IgG based SAMs covering a gold working electrode in a standard three electrodes cell, are shown to be permeable to the ferro/ferricyanide $[Fe(CN)_6]^{3-/4-}$ redox probes. These ions can reach the gold surface and undergo oxidation, even when the full bio-functionalization of the gate surface is accomplished. The SiMoT SAM capacitance/square was measured to be 10 μF/cm^2 [10] and the total SAM capacitance was estimated to be 3.3 μF. The IgM and IgG sensing is performed by measuring the SiMoT transfer characteristics after incubation for 10 min of the anti-IgM or the anti-IgG SAM in 100 μl PBS with osmolality and ion concentrations matching those of the human body (pH=7.4; ionic-strength=162 mM). The gate was washed thoroughly with HPLC-water and placed in the SiMoT device. After the measurement of a stable I_0 base line (red-line **Figure 1E**), the same gate was immersed and incubated for 10 min in 100 μl of the PBS standard-solutions of the ligands (IgG or IgM) with nominal concentrations ranging from 6 zM to $60\cdot10^8$ zM. After each incubation, the SAM was washed thoroughly with water to remove the unreacted ligands and further I-V transfer curves were measured. The sensing curves, measured after incubation of the same anti-IgM functionalized gate into progressively more concentrated IgM standard-solutions in PBS, are shown in **Figure 1E.** The black-curve in **Figure 1E** is relevant to the incubation of the same gate in the 6 zM solution. It shows no change compared to the base line as in 100 μl at 6 zM Poisson sampling foresees a 68.3% probability that no IgM is present. The blue-curve, measured at 60 zM concentration shows, over tens of replicates, a significant current decrease as well as a shift towards more negative gate potentials. A change here is also expected as the Poisson sampling foresees that 4 ± 2 ligands are found in 100 μl (error taken as the square root of the number of molecules). Hence at least 2 ligands are always found in 100 μl at 60 zM. A further current decrease is measured at higher concentrations and similar data are gathered for the IgG measured with an anti-IgG SAM. Importantly, before and after the sensing, a control experiment is always accomplished, placing a bare gold gate on top of the P3HT resistor and measuring the transfer characteristics. If comparable current levels (within 8 %) are measured, the data set is accepted. The logarithmic plot of the transfer characteristics is given in **Figure 5S**. These curves show that, upon binding, an appreciable shift of V_T towards more negative values, occurs. This is ascribed to an electrostatic change, namely a variation of the surface dipole moment possibly due to a change in the H-bond structure.[10] Such an electrostatic change could be measured as the charge double layer formed at the interface between the SAM and the water upon application of the gate bias was largely unscreened. Indeed, the device was operated in deionized water and the Debye length λ_D was above 100 nm hence much larger than the whole SAM (~ 6 nm).

The relative current change upon exposure of the SAM to the ligands in the PBS solutions, $\Delta I/I_0 = [(I-I_0)/I_0]$, is the SiMoT sensing response. The "I" values at each concentration are taken from the relevant transfer curves (**Figure 1E**) at the V_G that maximises the trans-conductance $g_m=\delta I_D/\delta V_G$. This V_G value falls generally between - 0.25 V and - 0.35 V. The $\Delta I/I_0$ *vs.* IgM concentrations dose curve measured with the anti-IgM and BSA functionalized gate are shown in **Figure 2A** as red squares, while the black circles are the negative control responses measured exposing the anti-IgM functionalized gate to IgG. The zero response of anti-IgG to IgM proves that the anti-IgM SiMoT device is indeed selective to IgM. In **Figure 2B** the sensing data of IgG with an anti-IgG based SAM is shown (red squares) while the black circles are the data of the control experiment with IgM. Similarly, these data prove the high selectivity of the anti-IgG SiMoT to IgG. The blue diamonds belong to the IgG dose curve measured on the anti-IgG based SAM that does not comprises any physisorbed BSA. All the data points, both in **Figure 2A** and **2B**, are the average over three replicates measured on different gates and different transistors. Error bars are taken as one standard

deviation, indicating a good inter-device reproducibility, and the full lines are the result of the SiMoT dose-curve modelling that will be discussed later. The limit of detection (LOD) level was computed as the concentration providing a response equal to the average of the noise level of the negative control data in the whole concentration range plus three times the noise' standard-deviation.[6] The LOD level for the IgG sensing with the SAM comprising both anti-IgG and BSA is at 15% and the data modelling curve enables to correlate this to a concentration of 11 zM. The number of IgGs at the LOD is equal to $[c]\cdot V\cdot N_A$, with $[c] = 10.7\cdot10^{-21}$ mol·l^{-1}, V = 100µL, N_A = Avogadro's number. So this corresponds to a LOD of 1±1 molecule. The LOD increases to 2.5 aM (160±13 molecules) when no BSA is added, showing that the BSA is needed to reach the single-molecule limit. A LOD of aM was also measured by means of an organic electrochemical transistor with an anti-IgG functionalized gate also not comprising any adsorbed BSA.[12] Such an evidence confirms the critical role of the BSA in reaching detection level. On the other hand, it also shows that organic electrochemical transistors, usually measuring in the pM-nM range at most, can perform at ultra-low detection limits. The LOD level for the IgM sensing, falling at 12%, also demonstrates that single molecule detection is achieved. The dose curves in **Figure 2A** and **2B**, all together show that single molecule detection can indeed be achieved with a wide-field millimetre-size transistor and also, for the first time, it is shown that a high selective detection of proteins such as IgG and IgM is possible in a physiologically relevant environment.

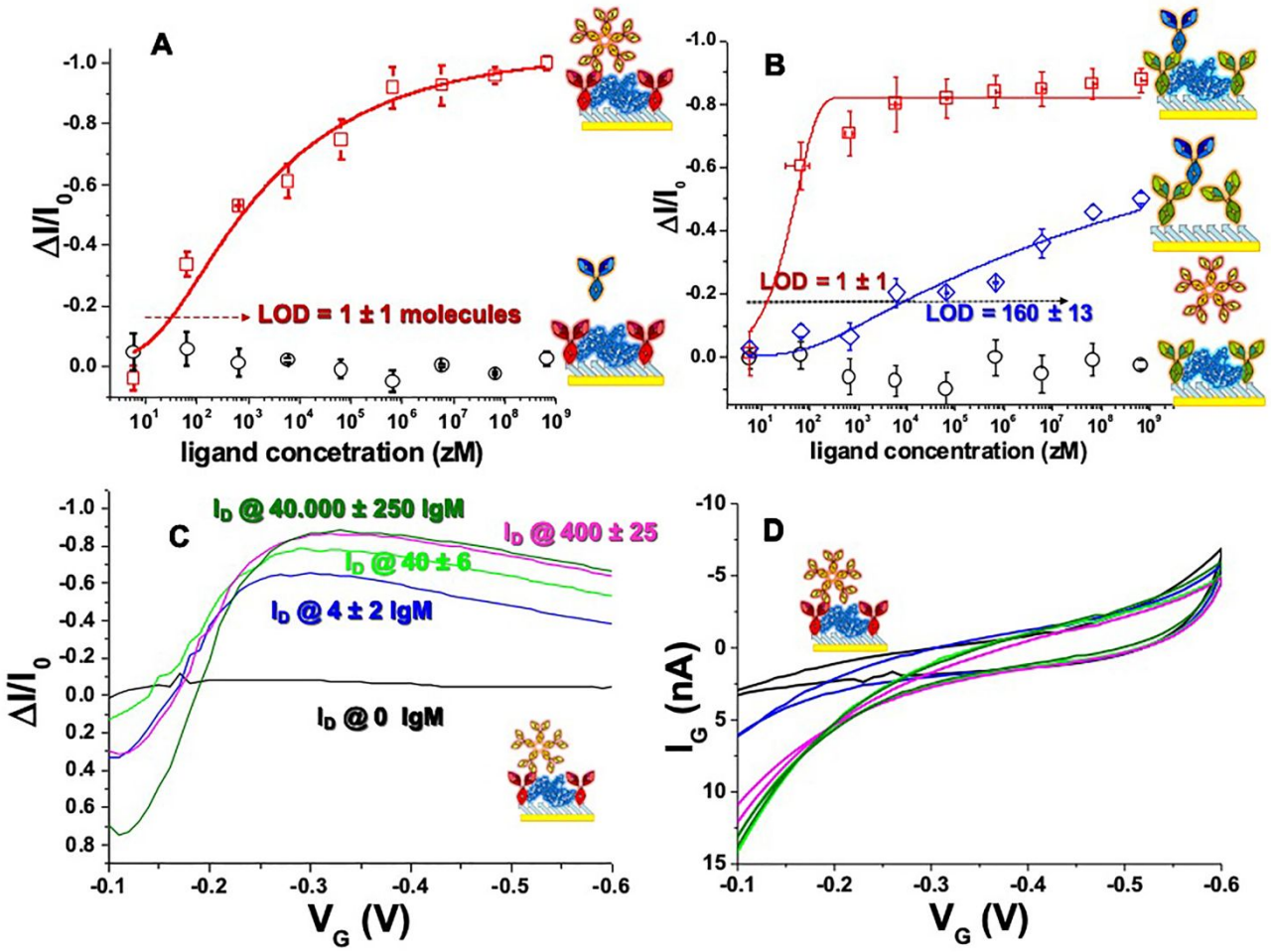

Figure 2. A - IgM/anti-IgM affinity binding calibration-curve (red-squares) are shown as the relative change of the I_D current ($\Delta I/I_o$) vs. the IgM concentration. A functionalized gate comprising both the anti-IgM and the BSA is used. The black-circles are the negative control responses of the anti-IgM to IgG solutions. **B** - IgG/anti-IgG affinity binding calibration-curve (red-squares) as the relative change of the I_D current ($\Delta I/I_o$) vs. the IgG concentration. A functionalized gate comprising both the anti-IgG and the BSA is used. The black-circles are the negative control responses of the anti-IgG to IgM solutions. The blue diamonds belong to the dose curve measured on the anti-IgG SAM that does not comprises the BSA blocking layer. **C** - $\Delta I/I_o$ of I_D vs. V_G at V_D = -0.4 V for IgM molecules ranging from 0 to $6\cdot10^4$. The data are the same as in panel A. **D** - Gate leakage current, I_G, vs. V_G as a function of IgM detected concentrations. The concentrations are marked with the same colour code as in panel **C**.

The data here presented are a proof-of-principle but they can be considered as relevant for future perspective applications in the selective detection at the physical limit of immunoglobulins that can simulate the anti-dengue virus IgG

and IgM. As for all the infection diseases, early diagnosis is of high importance to stop the spreading. It is in fact known that the first days after the infection are the most dangerous due to the virulence of the infection. For example, Dengue infection is ranked as a major public health concern and there is still no licensed vaccine or antiviral drug available for its prevention and treatment.[17]

Interesting is to comment the $\Delta I/I_0$ SiMoT sensing response dependence from V_G shown in **Figure 2C**. These data prove that, above the threshold voltage ($V_T \sim$ - 0.2V), the sensing response increases with the concentration of the cognate ligand and the maximal response is in the same V_G range where also g_m is maximized. However, the correlation between the SiMoT response and the ligand concentration is lost below V_T. This is important because below V_T the I_D current measured is due to leakage (current not due to capacitive coupling between the gate and the channel likely associated with the organic semiconductor not being confined in the channel region) and hence there is no more field-effect induced on-current flowing. **Figure 2D** shows also no apparent correlation between the I_G current level (also not field-induced) and the ligand concentration. These are compelling evidences, very seldom provided when transistor sensors are proposed, proving that the field-effect induced current I_D provides a field-effect amplified sensing response quantified as its fractional change. No other current flowing in the device can provide the same information. In the SiMoT configuration this is uniquely accomplished mostly because of two reasons: - the SAM of capturing protein and the electronic channel are coupled via a good electronic insulator as no electrochemical reaction takes place; - the sensing process directly affects the interfacial gating charge double layer and hence the I_D current flowing in the transistor channel.

DISCUSSION

Important at this point is to add pieces of information to the understanding on why a *wide-field* device can detect a protein at the physical limit. It has been already pointed out that the presence of the BSA in the SAM is necessary. Another relevant aspect is added by the IgG sensing performed on the gate where the anti-IgG and BSA are both physically adsorbed directly on gold, *i.e.* without the chem-SAM. While these data have been already proposed,[10] here they are discussed against a different control experiment (*vide infra*) and hence they provide a different information. The sensing curve, shown in **Figure 3A** (red squares), proves that the LOD is 30 aM ($2.4 \cdot 10^3$ bio-markers). This increase by three orders of magnitude proves that the chemical SAM is essential for the single-molecule sensing too. To better understand which property of the chem-SAM is relevant, we decided to test a SAM that is not electrostatically connected via an H-bonds network. Given that in the SiMoT device ~10^{12} capturing proteins are immobilized on the 3-MPA and 11-MUA chem-SAM, it can be estimated that there is one capturing protein per 10-100 11-MUA chains as alkanethiols packing on gold is $7.6 \cdot 10^{-10}$ mol·cm^{-1}. [18] Hence, the 11-MUA, being the longer and more flexible component of the mixed chem-SAM and being already sufficiently numerous, are more likely than the 3-MPA to conjugate the capturing antibodies. To tailor a system having a similar SAM that lacks, however, the H-bonds network the 3-MPA chains were substituted with 2-mercaptoethanol (2-ME) ones. The 11-MUA and 2-ME (1:10) chem-SAM is characterized by the absence of carboxylic groups on the shorter chains but the capturing proteins can still attach to the gate via the 11-MUA. In **Figure 2S** it is proven that still 10^{12} antibodies are attached to the gate when 2-ME are used. This is further supports the model that mostly the 11-MUAs are engaged with the conjugation of the capturing proteins. At the same time, the ethanolamine chemical blocking cannot generate an amide-based H-bonds network between two contiguous 2-MEs as there are no carboxylic groups available. The black circles in **Figure 3A** show that no sensing at all is measured when the 2-ME and 11-MUA chem-SAM lays underneath the anti-IgG and BSA bio-SAM.

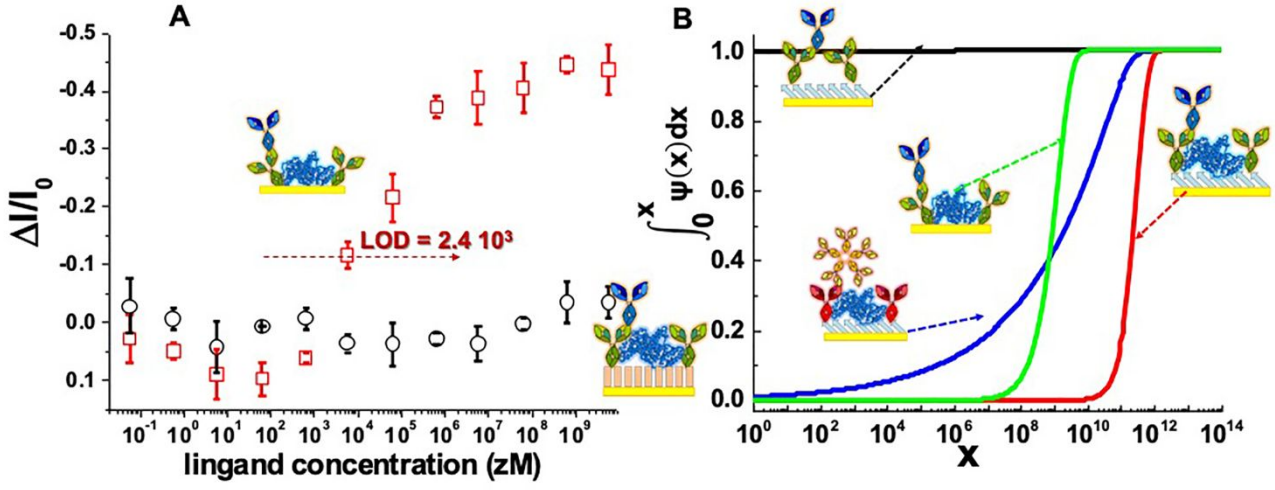

Figure 3. A IgG/anti-IgG affinity binding calibration-curve (red squares) as the relative change of the I_D current ($\Delta I/I_o$) vs. the IgG concentration. A functionalized gate comprising physical adsorbed anti-IgG blocked with the BSA is used. The black circles belong to the dose curve measured on the chem-SAM comprising 2-ME and 11-MUA (10:1). **B** – *The* $\int_0^x \Psi(x)dx$ vs. the number x of binding sites in a domain is shown. The Ψ(x) values are evaluated according to **[Eq. (5)]** using the best fit parameters for a given

dose curve, specifically: - IgM/anti-IgM bio-SAM (blue curve, data from **Figure 2A**);- IgG/anti-IgG bio-SAM (red curve, data from **Figure 2B**);- IgG/anti-IgG bio-SAM not comprising BSA (black curve, data from **Figure 2B**); - IgG/anti-IgG bio-SAM directly physisorbed on gold (green curve, data from **Figure 3A**).

This proves the critical role of the H-bonding network in the SiMoT approach. Interestingly, when the 2-ME is interfaced between the bio-SAM and the gold surface even the detection at the aM level, seen on the physisorbed capturing layer, is lost. This can be tentatively explained by considering that a chem-SAM with no H-bond network can disrupt the electrostatic coupling between the gold and the bio-SAM. Such an occurrence was proven true in a study carried out on stratified self-assembled structures endowed with H-bond interactions between different layers.[19] Moreover, 2-ME has been used as a diluent to block any exposed Au surfaces and minimize non-specific binding.[20]

To model such a system, it is assumed that the SAM on the gate is divided into a number of domains in which the capturing antibodies are highly densely packed (10^4 per μm^2) and electrostatically connected through an H-bond network. This network is present both in the chem-SAM and in the bio-SAM. The degree of electrostatic connection between the capturing antibodies within a domain is larger when the BSA is physisorbed. Each domain in the SAM is characterized by the following feature: if one cognate ligand (the bio-marker to be detected) binds to any of the capturing antibodies populating the domain, the entire domain changes its work-function due to a collective phenomenon. Cooperative interactions enabled by the hydrogen bonding network, serve to this scope. The process is assumed to be also irreversible so as no other change in work-function is possible, within that domain, if other affinity bindings occur. The propagation of the work-function change needs a compact, uniform and electrostatically connected SAM because the presence of a defect will stop the propagation and limit the domain. The more compact and defect-free the SAM is, the larger the domain generated upon interaction with one ligand is, the higher the sensing response will be. This is assumed to be the amplification process that, along with the proven field-effect amplified response, makes the single-molecule detection possible with the wide-field SiMoT sensor. With this picture in mind, a stochastic distribution of ligands on the gate area is considered. Since the gate is uniformly covered by a number **n** $\sim 10^{12}$ of capturing proteins, the probability to find a cognate ligand (IgM or IgG) bound to a given capturing protein is **p**=1/n. Assuming that the N ligands in the solution are distributed uniformly over the gate, the average number of ligands per binding site is $\lambda = Np = N/n << \sqrt{n}$. Being p very small and n very large, the probability for a number k of cognate ligands to interact with binding sites, follows a Poisson distribution:

$$\boldsymbol{P_k = \frac{\lambda^k e^{-\lambda}}{k!}} \quad (1).$$

Analogously, the probability that a given binding site does not interact with any ligand is:

$$\boldsymbol{P_0 = e^{-\lambda}} \quad (2)$$

An x number of binding sites within a domain is considered. Under the assumption that the probability of interaction of each of the k ligands, with each of the x capturing sites within that domain is mutually independent, the probability $f_o(x,\lambda)$ that none of these x binding sites interacts with anyone of the k ligands, is given by the product of the probabilities for each binding site to remain empty: $\boldsymbol{f_0(x,\lambda) = \prod_1^x P_0 = P_0^x = e^{-\lambda x}}$. To handle the case of domains having different sizes and hence are populated by a different number of ligands, the probability distribution function of the number of binding sites x in each domain $\Psi(x)$ is introduced. The total probability of finding a domain of capturing proteins that has not interacted with any of the N ligands present in the incubation volume V is:

$$\boldsymbol{f_0(\lambda) = \int_1^n \Psi(x) f_0(x,\lambda) dx = \int_1^n \Psi(x) e^{-\lambda x} dx \approx}$$

$$\boldsymbol{\int_0^\infty \Psi(x) e^{-\lambda x} dx} \quad (3)$$

where the upper limit of integration, $\boldsymbol{n} = 10^{12}$, has been approximated to infinite and the lower one to zero. The probability $f_o(x,\lambda)$ in **[Eq. (3)]** is, hence, the Laplace Transform of the distribution function of the number of binding sites of a given domain $\Psi(x)$. So, the probability that one ligand binds to one capturing protein in a domain is: $\boldsymbol{f_{k\geq 1}(\lambda) = 1 - f_0(\lambda)}$. It is further assumed that each data point in a given $\Delta I/I_0$ dose curve is proportional to the number of domains in which the work-function has been changed by the binding with one ligand, hence:

$$\boldsymbol{\frac{\Delta I}{I_0} = A_{sat}(1 - f_0(\lambda))} \quad (4).$$

where A_{sat} is the $\Delta I/I_0$ saturation level while the dependence of λ on the ligands molar concentration [c] in a sampled solution of volume V is: $\lambda = [c]\cdot V\cdot N_A\cdot n^{-1}$. The unknown $\Psi(x)$ distribution is assumed to be a unimodal gamma-distribution:[21]

$$\boldsymbol{\Psi(x) = \frac{x^{b-1} exp\left(-\frac{x}{K}\right)}{K^b \quad \Gamma(b)}} \quad (5).$$

where $\Gamma(b)$ is the gamma function, b is the characteristic shape and K the scale parameters correlated to the distribution mean as $\boldsymbol{\bar{x} = Kb}$ and to the variance as $\boldsymbol{\sigma^2 = bK^2}$. A definite mode exists only for $b \geq 1$ and equals (b-1)K. The gamma-distribution Laplace transforms in the λ-domain is:

$$\boldsymbol{f_0(\lambda) = (1 + K\lambda)^{-b}} \quad (6)$$

Rearranging **[Eq. (6)]** and expressing the b and K parameters as a function of $\bar{x}$ and σ^2 respectively, the SiMoT model for the experimental dose-response curves becomes:

$$\frac{\Delta I}{I_0} = A_{sat}\left(1 - \left(1 + \frac{\sigma^2}{\bar{x}} \cdot \frac{c \cdot V \cdot N_A}{n}\right)^{-\left(\frac{\bar{x}}{\sigma}\right)^2}\right) \quad (7).$$

Fitting **[Eq.(7)]** to the dose curves results in the sold lines of **Figure 2A**, **Figure 2B** and **Figure 3A**. Indeed, the SiMoT analytical model very well reproduces the experimental data. The best-fit values for IgG/anti-IgG curve (red squares in **Figure 2B**) are $\bar{x} = 3 \cdot 10^{11}$ and $\sigma = 7 \cdot 10^5$ and $\bar{x} = 3 \cdot 10^7$ and $\sigma = 5 \cdot 10^9$ for IgG/anti-IgG without BSA (blue triangles in **Figure 2B**). These values in **[Eq. (5)]**, reveal the $\Psi(x)$ distribution for a given SAM. The lower-tail cumulative distributions, $\int_0^x \Psi(x)dx$, giving the probability of a domain to comprise less that x binding sites, are shown in **Figure 3B**. For the IgG/anti-IgG sensing on the bio-SAM including BSA (red curve) nearly monodispersed giant domains are revealed so as there is 100% probability of finding domains smaller than $1.3 \cdot 10^{12}$ anti-IgG capturing sites. Conversely, without BSA (black curve) the domains generated in the SAM are very much dispersed, even containing one single binding site. In any case some rather large domain is still possible hence the LOD is fairly high, but not sufficiently high to enable single molecule detection. Likely BSA occupies defect states making the SAM more compact. When the IgG/anti-IgG sensing is carried out on the physisorbed SAM (green curve, $\bar{x} = 1 \cdot 10^9$ and $\sigma = 1 \cdot 10^9$) there is 100% probability of finding domains populated by less than $9 \cdot 10^9$ capturing antibodies, hence three orders of magnitude smaller than the SAM comprising the functioning chem-SAM. Interesting is the case of the IgM/anti-IgM that reveals a broad distribution of domain size (blue curve, $\bar{x} = 1.7 \cdot 10^{11}$ and $\sigma = 4 \cdot 10^{11}$). Similar to the case of the IgG/anti-IgG there is 100% probability of finding large domains of $5 \cdot 10^{11}$ anti-IgM but there is also a rather large probability of finding much smaller ones. This explains why single molecule detection is possible also in this case although the dose curve response is much smoother. This suggests that the anti-IgG and anti-IgM SAMs are characterized by very different electrostatic coupling and/or number of defects, but will need further dedicated in-depth studies to be fully understood.

In conclusion this work shows that the single-molecule label-free sensing of immunoglobulins performed with a large SiMoT bioelectronic sensor, that is not only extremely sensitive but also highly selective. The role of the capturing bio-SAM compactness as well as that of the H-bonding network characterizing the chem-SAM enable detections at the physical limit, are discussed too. The single-molecule transistor dose curve modelling involves the two-dimensional Poisson distribution that sheds light on the sensing mechanism. Perspective applications in the early detection of infection diseases are foreseen.

ASSOCIATED CONTENT

Supporting Information

P3HT SiMoT stability, angular response of the conjugation of the anti-IgM and anti-IgG antibodies to the activated 3-MPA and 11-MUA chem-SAM as a function of time, angular response of the conjugation of the anti-IgG antibodies to the activated 2-ME and 11-MUA chem-SAM as a function of time, cyclic voltammograms for anti-IgM and anti-IgG bio-SAMs on gold working electrodes, logarithmic version of the transfer curves given in **Figure 1E** to better highlight the threshold voltage shift at progressively higher IgM concentrations.

The Supporting Information is available free of charge on the ACS Publications website.

AUTHOR INFORMATION

Corresponding Author

* e-mail: luisa.torsi@uniba.it

Author Contributions

E.M fabricated the devices and measured the single-molecule sensing in PBS and in real fluids. A.T. fabricated the devices and measured the single molecule sensing in PBS. K.M. and B.H. characterized the gates by electrochemical and surface plasmon resonance measurements. N.D. contributed to the surface characterization of the bio-functionalized gates. R.A.P. studied the stability of the devices. N.C. supervised the electrochemical characterization and stability of the devices. C.DF. fabricated the source and drain interdigitated patterns. G.S. supervised the micro-fabrication of the devices and the morphological characterization of the bio-functionalized gates. G.P. conceived and produced the dose-curve model based on the Poisson statistics. L.T. conceived the idea of the SiMoT device, coordinated the team and wrote the manuscript that was revised and approved by all the authors.

ACKNOWLEDGMENT

We thank F. Torricelli, P. Romele, G. Mangiatordi, D. Albenga and R. Osterbacka, for useful discussions. “OrgBIO” Organic Bioelectronics (PITN-GA-2013-607896), PON SISTEMA (MIUR), Future in Research “FLOW” Dispositivi EGOFET flessibili a bassa tensione per la sicurezza in campo alimentare (Codice Pratica: ML5BJ85) and Fondo di Sviluppo e Coesione 2007-2013 – APQ Ricerca Regione Puglia “Programma regionale a sostegno della specializzazione intelligente e della sostenibilità sociale ed ambientale - FutureInResearch” - “BEND” Biosensori elettronici intelligenti per la diagnosi precoce di malattie neurodegenerative (B164PG8) projects and CSGI are acknowledged for partial financial support.

REFERENCES

[1] J. Gooding, K. Gaus, Single molecule sensors: challenges and opportunities for quantitative analysis. *Angew. Chem. Int. Ed.* **2016**, *55*, 11354.

[2] L. Q. Gu, J. W. Shim, Single molecule sensing by nanopores and nanopore devices. *Analyst* **2010**, *135*, 441.

[3] S. Sorgenfrei, C.Y. Chiu, Jr. R.L. Gonzalez, Y.J. Yu, P. Kim, C. Nuckolls, K.L. Shepard, Label-free single-molecule detection of DNA-hybridization kinetics with a carbon nanotube field-effect transistor. *Nature Nanotechnology* **2011**, *6*, 126-132.

[4] T. A. Dickinson, J. White, J. S. Kauer, D. R.Walt, A chemical-detecting system based on a cross-reactive optical sensor array. *Nature* **1996**, *382*, 697.

[5] D. M. Rissin, C. W. Kan, T. G. Campbell, S. C. Howes, D. R. Fournier, L. Song, T. Piech, P. P. Patel, L. Chang, A. J. Rivnak, E. P. Ferrell, J. D. Randall, G. K. Provuncher, D. R. Walt, D. C. Duffy, Single-molecule enzyme-linked immunosorbent assay detects serum

proteins at subfemtomolar concentrations. *Nat. Biotechnol*. **2010**, 28, 595.
[6] M. Thompson, S.L.R. Ellison, R. Wood, Harmonized guidelines for single-laboratory validation of methods of analysis (IUPAC Technical Report). *Pure Appl. Chem.* **2002**, *74*, 835.
[7] S. Chen, M. Svedendahl, R. P. Van Duyne, M. Kall, Plasmon-enhanced colorimetric ELISA with single molecule sensitivity. *Nano Lett.* **2011**, *11*, 1826.
[8] E. Macchia, K. Manoli, B. Holzer, C. Di Franco, M. Ghittorelli, F. Torricelli, D. Alberga, G. F. Mangiatordi, G. Palazzo, G. Scamarcio, L. Torsi, Single-molecule detection with a millimetre-sized transistor. *Nature Communications* **2018**, 3223, DOI: 10.1038/s41467-018-05235-z.
[9] A sensor detects the light touch of a single molecule. Nature Research Highlight 16.08.2018 https://www.nature.com/articles/d41586-018-05950-z
[10] K. Manoli, M. Magliulo, M.Y. Mulla, M. Singh, L. Sabbatini, G. Palazzo, L. Torsi, Printable bioelectronics to investigate functional biological interfaces. *Angew. Chem. Int. Ed.* **2015**, *54*, 2.
[11] A. Balmaseda, M. G. Guzman, S. Hammond, G. Robleto, C. Flores, Y. Tellez, E. Videa, S. Saborio, L. Perez, E. Sandoval, Y. Rodriguez, E. Harris, Diagnosis of dengue virus infection by detection of specific immunoglobulin M (IgM) and IgA antibodies in serum and saliva. *Clinic. Diagnos. Lab. Immunol.,* **2003**, *10*, 317.
[12] E. Macchia, P. Romele, K. Manoli, M. Ghittorelli, M. Magliulo, Z. M. Kovàcs-Vajna, F. Torricelli, L. Torsi, Ultra-sensitive protein detection with organic electrochemical transistors printed on plastic substrate. *IOP Flexible and Printed Electronics* **2018**, 3:034002**.**
[13] J. C. Thomas, D. P. Goronzy, K. Dragomiretskiy, D. Zosso, J. Gilles, S. J. Osher, A. L. Bertozzi, P. S. Weiss, Mapping Buried Hydrogen-Bonding Networks. *ACS Nano* **2016**, 10, 5446.
[14] B. Holzer, K. Manoli, N. Ditaranto, E. Macchia, A. Tiwari, C. Di Franco, G. Scamarcio, L. Torsi, Characterization of Covalently Bound Anti-human Immunoglobulins on Self-assembled Monolayer Modified Gold Electrodes. *Advanced BioSystems* **2017**, 1700055, 1.
[15] E. Perlmann, L. G. Longsworth, The specific refractive increment of some purified proteins. *J. Am. Chem. Soc.* **1948**, 70, 2719.
[16] H. Zhao, P.H. Brown, P. Schuck P., On the distribution of protein refractive index increments. *Biophysical Journal* **2011**,100, 2309.
[17] O. Parkash and R. H. Shueb, Diagnosis of Dengue Infection Using Conventional and Biosensor Based Techniques. *Viruses* **2015**, 7, 5410.
[18] C.A. Widring, C. Chung, M.D. Porter, The electrochemical desorption of n-alkanethiol monolayers from polycrystalline Au and Ag electrodes. *J. of Electroanal. Chem*. **1990**, 310, 335.
[19] R.S. Clegg, S.M. Reed, R.K. Smith, B.L. Barron, J.A. Rear, J.E. Hutchison, The interplay of lateral and tiered interactions in stratified self-organized molecular assemblies. *Langmuir* **1999**, 15, 8876.
[20] H. Trzeciakiewicz, J. Esteves-Villanueva, R. Soudy, K. Kaur, S. Martic-Milne, Electrochemical Characterization of Protein Adsorption onto YNGRT-Au and VLGXE-Au Surfaces. Sensors 2015, 15, 19429.
[21] E.W. Weisstein, in CRC Concise Enciclopedia of Mathematics, Chapman & Hall/CRC, New York, USA 1999, p. 69.

Table of Contents

Selective single-molecule detection of IgM and IgG mutually interacting with anti-IgM or anti-IgG capturing antibodies, are measured with a large-area organic bio-electronic device. A model based on the Poisson distribution well reproduces the dose curves and provides a model for the single-molecule sensing mechanism. Perspective applications are in the early detection of infection as well as progressive diseases.